US–FT/16–94

Strangeness enhancement and string fusion in nucleus–nucleus collisions

N. Armesto, M. A. Braun[1], E. G. Ferreiro and C. Pajares
Departamento de Física de Partículas,
Universidade de Santiago de Compostela,
15706–Santiago de Compostela, Spain

Abstract

In a Monte Carlo code based on the Quark Gluon String Model it is shown that the fusion of strings produces an enhancement of Λ, $\overline{\Lambda}$ and ϕ production, and a reduction of K^- production and total multiplicities. The results are in reasonable agreement with most of the experimental data for hadron–hadron, hadron–nucleus and nucleus–nucleus collisions, especially with the large $\overline{\Lambda}$ enhancement which is well reproduced. Predictions for Pb–Pb collisions at $p_{lab} = 200\ GeV$ per nucleon are also presented.

US–FT/16–94
October 1994

[1] On leave of absence from the Department of High Energy Physics, University of St. Petersburg, 198904 St. Petersburg, Russia.

1. Introduction: The Dual Parton Model (DPM) ([1]) or equivalently the Quark Gluon String Model (QGSM) ([2]) and models based on them like VENUS ([3]) have been very successful in describing particle production in hadron–hadron, hadron–nucleus and nucleus–nucleus interactions. Monte Carlo versions of these models ([3, 4, 5, 6]) are in reasonable agreement with most of the properties of soft multiparticle production.

Enhanced generation of strange particles ([7, 8, 9, 10, 11, 12]), in particular of strange antibaryons and ϕ–mesons, has been observed in recent experiments at the CERN SPS. This enhanced production is not explained in the models quoted above ([3, 4, 6]) and may be a possible signal of the formation of Quark Gluon Plasma (QGP) ([13]). However it is worth to pursue the study of modifications of the conventional models without QGP formation before drawing final conclusions. In this way, in the DPM the creation of sea diquark–antidiquark pairs from the vacuum has been introduced, in addition to the usual quark–antiquark pairs ([14]). The rate of diquark–antidiquark production as compared to the quark–antiquark one is assumed to be the same as in string fragmentation. Besides, in the DPM the so–called popcorn mechanism of diquark fragmentation has been included. A detailed comparison with the experimental data is done in this reference. Creation of strange quarks from the sea (at the same rate as in string fragmentation) is also considered.

In VENUS the fusion of particles and resonances into large clusters which decay isotropically ([15]) has been introduced.

In QGSM the fusion of strings has been incorporated. A first comparison with experimental data shows a qualitative agreement with most of them ([6]), however the new data of the NA35 Collaboration ([7]) show large differences. In this paper we re–examine the situation changing the strength of the fusion of strings. We do not introduce either cascading or the popcorn mechanism ([14]), although in principle they should be present. The reason for this is that we are not looking for a perfect fit but just to understand in a clean and clear way what are the effects of each separate mechanism. We know that the main effects of cascading are: 1) A moderate increase of multiplicities in the fragmentation region of the nucleus, 2) A shift of baryons towards the central region, 3) The production of K^+, $\overline{K^0}$ and Λ due to the processes

$\pi^-\mathrm{p}(\pi^0\mathrm{n}) \to K^+\Sigma^-, \overline{K^0}\Lambda$; $\pi^+\mathrm{n}(\pi^0\mathrm{p}) \to K^+\Sigma^0, K^+\Lambda, \overline{K^0}\Sigma^+$;

$\pi^+\mathrm{p} \to K^+\Sigma^+$ and $\pi^-\mathrm{n} \to \overline{K^0}\Sigma^-$,

4) A decrease of K^- and K^0 due to the processes

$K^-p \rightarrow \pi^0\Lambda$, $\pi^+\Sigma^-$ and $K^-n \rightarrow \pi^0\Sigma^-$

and 5) An increase of ϕ production due to the processes

$K^+\Lambda \rightarrow \phi p$ and $K^+K^- \rightarrow \phi\pi^0$.

We also know that the popcorn mechanism shifts baryons towards the central rapidity region and produces a further enhancement of strange baryons. Therefore, when comparing the results of string fusion with experimental data we have to be aware of the lack of these two effects.

2. The Monte Carlo String Fusion Model: A detailed description of the Monte Carlo String Fusion Model (including the string fusion mechanism) together with a detailed comparison with experimental data can be found in Ref. [6].

It is assumed that strings fuse when their transverse positions come within a certain interaction area a. In the previous paper this area was taken the same as the parton–parton cross section $\sigma_p = 3.5\ mb$. However there is no reason for that. On the contrary, due to the fact that the strings are objects with structure, the string–string cross section is expected to be larger than the parton–parton one. In addition to this, in the Monte Carlo code we consider only fusion of two strings, but there is a probability of fusion of more than two. An effective way of taking it into account is to increase the cross section for the fusion of two strings. We will take $a = 7.5\ mb$. This larger value is crucial to improve the agreement with the strangeness enhancement shown by the data.

The fusion can take place only when the rapidity intervals of the strings overlap. It is formally described by allowing partons to interact several times, the number of interactions being the same for projectile and target. The quantum numbers of the fused string are determined by the interacting partons and its energy–momentum is the sum of the energy–momentum of the ancestor strings. The colour charges of the fusing string ends sum into the colour charge of the resulting string ends according to the $SU(3)$ composition laws. In particular, two triplet strings fuse into an antitriplet and a sextet string, with probabilities 1/3 and 2/3 respectively. A triplet and an antitriplet string give rise to a singlet state and an octet string with probabilities 1/9 and 8/9 respectively. In present calculations only fusion of two strings has been considered.

The breaking of the fused string is due to the production of two (anti)quark complexes with the same colour charges Q and $\overline{Q}$ as those at the ends of the string. The probability rate is given by the Schwinger formula ([16, 17, 18]):

$$W \sim K_{[N]}^2 exp(-\pi M_t^2/K_{[N]}) \ , \qquad (1)$$

where $K_{[N]}$ is the string tension for the $[N]$ $SU(3)$ representation proportional to the corresponding quadratic Casimir operator $C^2_{[N]}$. In our case

$$C^2_{[3]} = 4/3, \quad C^2_{[6]} = 10/3, \quad C^2_{[8]} = 3 \quad . \tag{2}$$

Therefore, the [8] and [6] fused strings have a larger string tension, giving rise to a larger heavy flavour production, in particular strangeness production.

The fundamentals of string fusion were introduced in Refs. [19] and [20] and the applications can be seen in Refs. [6] and [21].

3. p–p and p–A collisions: The parameters in the model were fitted to give a reasonable agreement with the data on proton–proton collisions. In Table 1 we show our results with and without string fusion together with the experimental data ([22]) at p_{lab} =200 GeV/c. A reasonable agreement is obtained, in particular for K^- and K^+. In this way the strangeness parameter λ_s is fixed. For Λ and especially for $\overline{\Lambda}$ our results are larger than the data. However at these energies the cross section for Λ and $\overline{\Lambda}$ production is rising very sharply due to the so–called delayed threshold effects ([23]). In the Monte Carlo code at these energies, with a very low number of strings (very close to two), the production rate for Λ's and $\overline{\Lambda}$'s turns out to be very sensitive to the details of energy division between partons and strings and of the mechanism for conversion of low–mass strings into hadrons. For that reason we prefer to compare our predictions for Λ and $\overline{\Lambda}$ production in hadron–hadron collisions at higher energies, with a larger number of strings formed. For p–$\overline{p}$ at $\sqrt{s}$=200 GeV our results are on satisfactory agreement with experimental data: we calculate $n_{\Lambda+\overline{\Lambda}}$=0.23 whereas the experiment gives $n_{\Lambda+\overline{\Lambda}}$=0.31±0.09 ([24]). Note that with nuclear targets or/and projectile the number of strings turns out to be much larger, so that the mentioned details average out and the comparison with experimental data at $\sqrt{s}$=20 GeV is more reliable.

In Table 2 our results on negative particles, K^0_S's and Λ's in proton–sulphur and proton–gold collisions at p_{lab} = 200 GeV/c per nucleon are shown. From this table it is seen that our multiplicities both with and without fusion are somewhat lower than the experimental data ([22]), especially for proton–gold collisions. For these we also obtain slightly less Λ's. These two effects, less multiplicities and less Λ's, will also be found in nucleus–nucleus collisions and can be accounted for by including cascading among secondaries and with spectators.

The number of $\overline{\Lambda}$'s turns out to be directly related with the string fusion probability: if the latter is reduced by a factor 2, as done in Ref. [6], the number of $\overline{\Lambda}$'s is also reduced a factor 2.

In Fig. 1a and 1b the rapidity distributions for K^0_S and Λ production are plotted for proton–gold collisions. It is seen that our results for Λ production are larger than the experimental data ([25]) in the extremes of the rapidity range and smaller in the center of the interval. This disagreement can be corrected by introducing the popcorn mechanism which transfers Λ's from the fragmentation region to more central rapidities. Cascading also helps, working in the same direction.

4. Central A–B collisions: In Table 3 our results for multiplicities of produced hadrons are shown for central ($b = 0$) S–S and S–Ag collisions at $p_{lab} = 200\ GeV/c$ without and with string fusion together with the experimental data ([10]). Rapidity distributions of K^0_S and $\overline{\Lambda}$ are presented in Figs. 2 and 3. It is seen that without string fusion a strong disagreement is observed for most data, especially for Λ, $\overline{\Lambda}$ and K^- production. In Λ production the ratio between the experimental data and results of the model without fusion is almost a factor 2 in S–S and S–Ag collisions. In K^- production the difference appears only in S–Ag. In $\overline{\Lambda}$ production the ratio is a factor 3. Inclusion of string fusion changes Λ and K^- production only slightly. However, the change is in the right direction: more Λ and less K^- are produced, but the results are still far from the experimental data. In both cases, as we mentioned, cascading is expected to produce more Λ particles and to reduce K^- production. This could be the reason of lesser differences in S–S than in S–Ag collisions. The popcorn mechanism would help to obtain a better agreement in the case of Λ production.

The case of $\overline{\Lambda}$'s is crucial to the study of the string fusion mechanism. Without it the experimental data are a factor 3 larger than the model predictions. Including string fusion an overall agreement is obtained. This can be seen in Fig. 3 where the experimental data ([7]) for $\overline{\Lambda}$ production in central S–S and S–Ag collisions are compared with the results without and with string fusion. Our results for $\overline{p}$ production in S–S and in S–Ag collisions are also presented. A strong increase is obtained in the case of fusion of strings with respect to the no fusion case.

In Table 3 we have also presented predictions for central Pb–Pb collisions. The main result that can be observed is a large enhancement for antibaryon production when we introduce string fusion (a factor 4 for $\overline{\Lambda}$'s and a factor 5 for $\overline{p}$'s). Rapidity

distributions of h^-, K^0_S and $\overline{\Lambda}$ for Pb–Pb collisions are presented in Fig. 4.

In Fig. 5 the NA38 experimental data ([11]) on the dependence of ϕ production on the energy density are compared with our results. It is seen that the string fusion enhances the ϕ production but the results still remain lower than the experimental data. However the rescattering in nucleus–nucleus collisions will enhance strongly ϕ production ([26]). Recently it has been argued that the enhancement depends only on the overlapping transverse area of the two nuclei ([12]). If this is confirmed, the cascade due to scattering of secondary hadrons with spectator nucleons would not be the origin of the enhancement, although rescattering of secondaries among themselves can not be ruled out.

5. Comparison with other models: Our results obtained with string fusion are similar to the ones recently obtained in the framework of the DPM including the creation of diquark–antidiquark pairs from the sea (the vacuum) in addition to the usual quark–antiquark pairs. In these results cascading and popcorn mechanism are also included ([14]). Probably this is the reason why a very good agreement with experimental data on Λ and K^- production was obtained. The $\overline{\Lambda}$ production agrees also with S–S and S–Ag experimental data and is a little over the S–Au data.

The DPM and the QGSM are essentially the same models. The inclusion in the first of the creation of diquarks–antidiquarks pairs of the sea is very similar to the inclusion of the fusion of strings in the QGSM. In fact, if in addition to diquark–antidiquark pairs (i. e.; 3–$\overline{3}$ colour pairs) more general pairs (qq) and $(\overline{qq})$ ($3 \otimes 3$ and $\overline{3} \otimes \overline{3}$ colour pairs) were allowed in the DPM the situation would be quite equivalent.

Concerning ϕ production, recently the experimental data have been explained ([27]) using the Relativistic Quantum Molecular Dynamics model (RQMD) ([28]), where fusion of strings is also included. The conclusion of this work is that 60 per cent of the experimentally observed rise is due to the fusion of strings and the rest is due to rescattering. This conclusion is in agreement with our results as it is seen in Fig 5. However the results of RQMD including fusion of strings in the case of $\overline{\Lambda}$ production ([29]) are smaller than our results and the experimental data.

6. Conclusions: Fusion of the strings produced in nucleus–nucleus interactions naturally explains the rise in strangeness as the multiplicity and centrality of the collision increase. The detailed results obtained in a Monte Carlo code based on the Quark

Gluon String Model show that the $\overline{\Lambda}$ enhancement experimentally observed and its rapidity distribution are well reproduced. Λ and ϕ enhancements are also produced by string fusion, but here additional mechanisms like rescattering of secondaries and popcorn are needed to obtain agreement with the experimental data. The production of K^- in S–Ag collisions results higher than the experimental data, even taking into account a small reduction due to string fusion. The effect of rescattering could reduce it down to an agreement with the data. Our results agree reasonably with the results of DPM on strangeness production and with the conclusion of the RQMD with string fusion on ϕ enhancement.

For all the reasons given above, we can conclude that the present experimental data on strangeness production can be explained by conventional models without formation of Quark Gluon Plasma, although in these conventional models unconventional collective mechanisms like string fusion are needed. The spectacular rise of $\overline{\Lambda}$'s and $\overline{p}$'s predicted in Pb–Pb collisions at $p_{lab} = 200\ GeV$ per nucleon can establish firmly the string fusion mechanism if it is confirmed by the new incoming experiments at SPS.

In conclusion we thank N. S. Amelin, A. Capella, M. Gazdzicki, C. Merino and J. Ranft for useful comments and a critical reading of the manuscript, and the CICYT of Spain for financial support. Also, N. A. and E. G. F. thank the Xunta de Galicia, and M. A. B. the Dirección General de Política Científica of Spain, for financial support.

References

[1] A. Capella, U. P. Sukhatme, C.–I. Tan and J. Tran Thanh Van, Phys. Rep. **236** (1994) 225.

[2] A. B. Kaidalov and K. A. Ter–Martirosyan, Phys. Lett. **B117** (1982) 247.

[3] K. Werner, Phys. Rep. **232** (1993) 87.

[4] H–J. Möhring and J. Ranft, Z. Phys. **C52** (1991) 643; I. Kawrakow, H. J. Möhring and J. Ranft, Z. Phys. **C56** (1992) 115.

[5] N. S. Amelin, L. P. Csernai, K. K. Gudina, V. N. Toneev and S. Yu. Sivoklolov, Phys. Rev. **D47** (1993) 1413.

[6] N. S. Amelin, M. A. Braun and C. Pajares, Phys. Lett. **B306** (1993) 312; Z. Phys. **C63** (1994) 507.

[7] NA35 Collaboration, presented by D. Röhrich at the QM93 Conference, Frankfurt preprint IFK–HENGPG/93–8 (1993) and Frankfurt preprint IFK–HENPG/94–1 (1994).

[8] E. Andersen *et al.*, Phys. Lett. **B316** (1993) 603.

[9] S. Abatzis *et al.*, Phys. Lett. **B270** (1991) 123.

[10] NA35 Collaboration, presented by M. Gazdzicki at the QM93 Conference, Frankfurt preprint IFK–HENGPG/93–6 (1993).

[11] R. M. Melo da Silva Ferreira, PhD. Thesis, Instituto Superior Tecnico, Lisbon (1993).

[12] C. Gerschel, in "The Heart of Matter", Rencontres de Blois, June 1994.

[13] J. Rafelski, Rencontres de Moriond (1993).

[14] J. Ranft, A. Capella and J. Tran Thanh Van, Phys. Lett. **B320** (1994) 346; private comunication (1994).

[15] K. Werner and J. Aichelin, Phys. Lett. **B308** (1993) 372.

[16] J. Schwinger, Phys. Rev. **82** (1951) 664.

[17] A. Casher, H. Neunberg and S. Nussinov, Phys. Rev. **D20** (1979) 179.

[18] M. Gyulassy and A. Iwazaki, Phys. Lett. **B165** (1985) 157.

[19] M. A. Braun and C. Pajares, Nucl. Phys. **B390** (1993) 542.

[20] M. A. Braun and C. Pajares, Phys. Lett. **B287** (1992) 154; Nucl. Phys. **B390** (1993) 559.

[21] N. S. Amelin, N. Armesto, M. A. Braun, E. G. Ferreiro and C. Pajares, Santiago preprint US–FT/3–94 (1994) (submitted to Phys. Rev. Lett.).

[22] M. Gazdzicki and O. Hansen, Nucl. Phys. **A528** (1991) 754; H. Bialkowska, M. Gazdzicki, W. Retyk and E. Skrzypczak, Z. Phys. **C55** (1992) 491.

[23] A. Capella, U. P. Sukhatme, C.–I. Tan and J. Tran Thanh Van, Phys. Rev. **D36** (1987) 109.

[24] R. E. Ansorge *et al.*, Z. Phys. **C41** (1988) 179.

[25] A. Bamberger *et al.*, Z. Phys. **C43** (1989) 25.

[26] P. Koch, O. Heinz and J. Pisut, Phys. Lett. **B243** (1990) 149.

[27] M. Berenguer, H. Sorge and W. Greiner, Phys. Lett. **B332** (1994) 15.

[28] H. Sorge, H. Stöcker and W. Greiner, Am. Phys. **192** (1989) 266; K. Sailer, T. Schönfeld, Z. Schram, A. Schäfer and W. Greiner, J. Phys. **617** (1991) 1005.

[29] H. Sorge, M. Berenguer, H. Stöcker and W. Greiner, Phys. Lett. **B289** (1992) 6.

Table Captions

Table 1. Comparison of experimental data ([22]) with the String Fusion Model code results, with and without string fusion, on average multiplicities of produced hadrons in proton–proton collisions at p_{lab} =200 GeV/c.

Table 2. Comparison of experimental data ([22]) with the the String Fusion Model code results, with and without string fusion, on the average number of negative particles (h^-), K^0_S's and Λ's in proton–sulphur and proton–gold collisions at $p_{lab} = 200$ GeV/c.

Table 3. Comparison of experimental data ([10]) with the String Fusion Model code results, with and without string fusion, on average multiplicities of produced hadrons in central AB collisions at $p_{lab} = 200$ GeV/c per nucleon for $S-S$ and $S-Ag$ collisions. Predictions for antiproton production in $S - S$ and $S - Ag$ collisions and for average multiplicities of produced hadrons in $Pb - Pb$ collisions are presented.

Figure Captions

Figure 1. Rapidity distributions in $p - Au$ collisions at $p_{lab} = 200\ GeV$ of: a) Λ's; b) neutral kaons. The experimental data (points with error bars) are from Ref. [25]. The results are obtained using the SFMC without string fusion (open symbols) and with fusion (black symbols).

Figure 2. Rapidity distributions of neutral kaons in central AB collisions at $p_{lab} = 200$ GeV per nucleon: a) $S - S$; b) $S - Ag$. The experimental data (points with error bars) are from Ref. [7]. The results are obtained using the SFMC without string fusion (open symbols) and with fusion (black symbols).

Figure 3. Rapidity distributions of $\overline{\Lambda}$'s in central AB collisions at $p_{lab} = 200\ GeV$ per nucleon: a) $S - S$; b) $S - Ag$. The experimental data (points with error bars) are from Ref. [7]. The results are obtained using the SFMC without string fusion (open symbols) and with fusion (black symbols).

Figure 4. Rapidity distributions of: a) h^-; b) K^0_S; c) $\overline{\Lambda}$ for central Pb–Pb collisions at $p_{lab} = 200\ GeV$ per nucleon. The results are obtained using the SFMC without string fusion (open symbols) and with fusion (black symbols).

Figure 5. Ratio $|\phi/(\rho + \omega)|_{\mu^+\mu^-}$ vs. energy density (in GeV/fm^3) in $p - W$ (first point on the left) and $S - U$ (all the other points) at $p_{lab} = 200\ GeV$ per nucleon. The experimental data (points with error bars) are from Ref. [11]. The results are obtained using the SFMC without string fusion (open symbols) and with fusion (black symbols). Only π^0 with $1.7 \leq \eta \leq 4.2$ and resonances with $3 \leq y \leq 4$ and $p_t \geq 0.6$ are accepted.

Table 1

	Experiment	Without fusion	With fusion
n_{ch}	7.69±0.06	7.50	7.34
n^-	2.85±0.03	2.75	2.67
K^+	0.28±0.06	0.29	0.29
K^-	0.18±0.05	0.18	0.19
K_s^0	0.17±0.01	0.23	0.22
π^0	3.34±0.24	3.15	3.00
π^+	3.22±0.12	3.17	3.06
π^-	2.62±0.06	2.51	2.38
Λ	0.096±0.01	0.20	0.19
$\overline{\Lambda}$	0.013±0.004	0.022	0.032
p	1.34±0.15	1.24	1.25
$\overline{p}$	0.05±0.02	0.051	0.070

Table 2

	Experiment	Without fusion	With fusion
Reaction	$p-S$	$p-S$	$p-S$
h^-	5.0±0.2	4.54	4.29
K_S^0	0.28±0.03	0.35	0.33
Λ	0.22±0.02	0.28	0.27
Reaction	$p-Au$	$p-Au$	$p-Au$
h^-	7.0±0.4	6.06	5.62
K_S^0	0.43±0.07	0.47	0.49
Λ	0.42±0.07	0.33	0.34

Table 3

	Experiment	Without fusion	With fusion
Reaction	$S-S$	$S-S$	$S-S$
n^-	95.5±5.0	99.6	90.3
Λ	8.2±0.9	4.4	4.8
$\overline{\Lambda}$	1.5±0.4	0.5	1.0
K_S^0	10.6±2.0	8.2	8.0
K^+	12.4±0.4	10.0	9.6
K^-	6.9±0.4	7.5	6.9
$\overline{p}$		0.9	3.0
Reaction	$S-Ag$	$S-Ag$	$S-Ag$
n^-	160.0±8.0	178.1	161.5
Λ	13.0±0.7	7.5	8.0
$\overline{\Lambda}$	2.4±0.4	0.8	1.8
K_S^0	13.2±1.1	14.9	14.3
K^+	17.4±1.0	17.3	16.7
K^-	9.6±1.0	13.6	12.4
$\overline{p}$		1.7	5.5
Reaction	$Pb-Pb$	$Pb-Pb$	$Pb-Pb$
n^-		924.4	806.2
Λ		32.8	41.9
$\overline{\Lambda}$		3.3	12.9
K_S^0		78.3	76.4
K^+		90.1	88.4
K^-		71.5	66.8
$\overline{p}$		6.7	35.5

Fig. 1

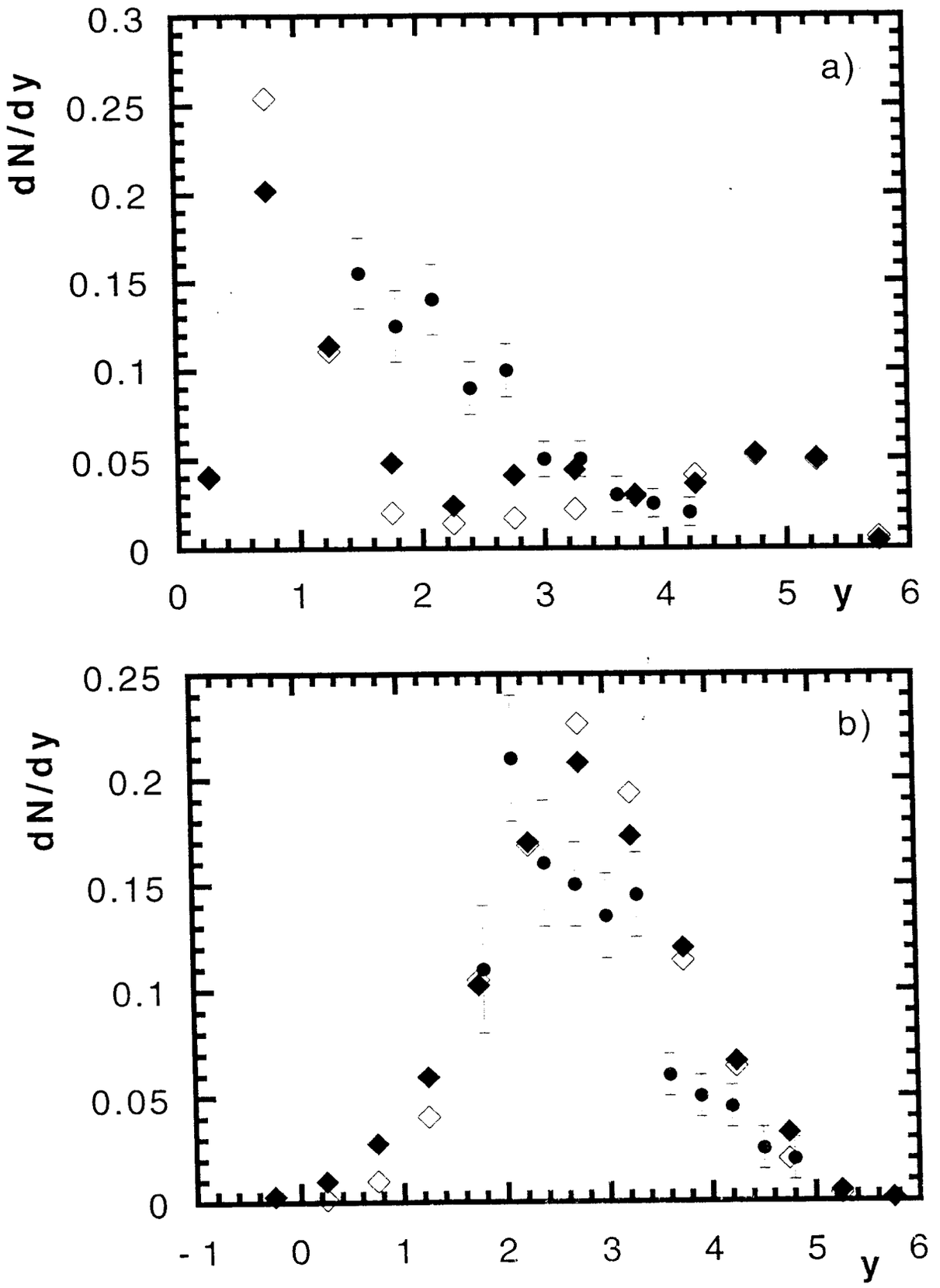
a)
dN/dy
0.3
0.25
0.2
0.15
0.1
0.05
0
0
1
2
3
4
5
y
6
b)
dN/dy
0.25
0.2
0.15
0.1
0.05
0
-1
0
1
2
3
4
5
y
6

Fig. 2

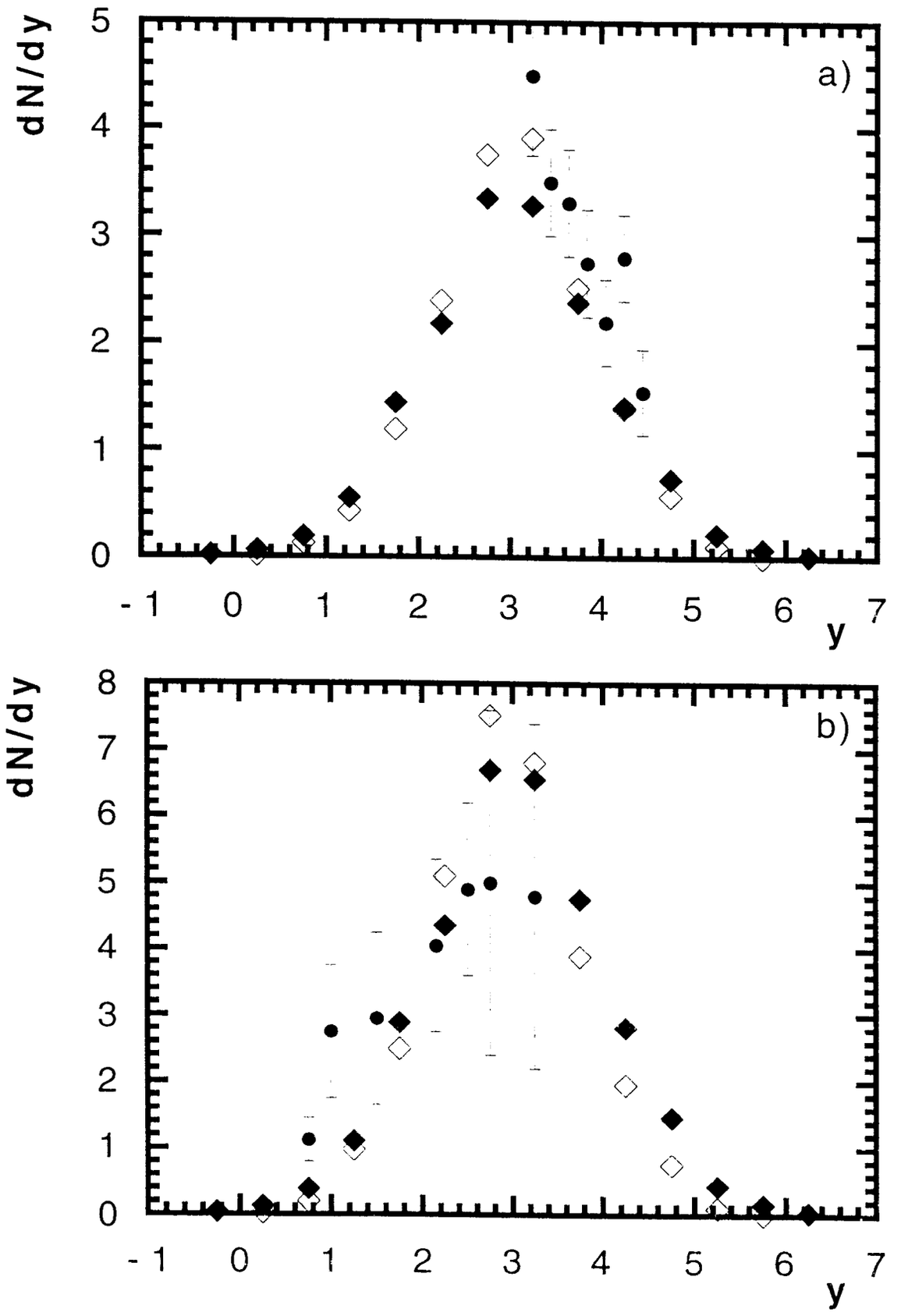

Fig. 3

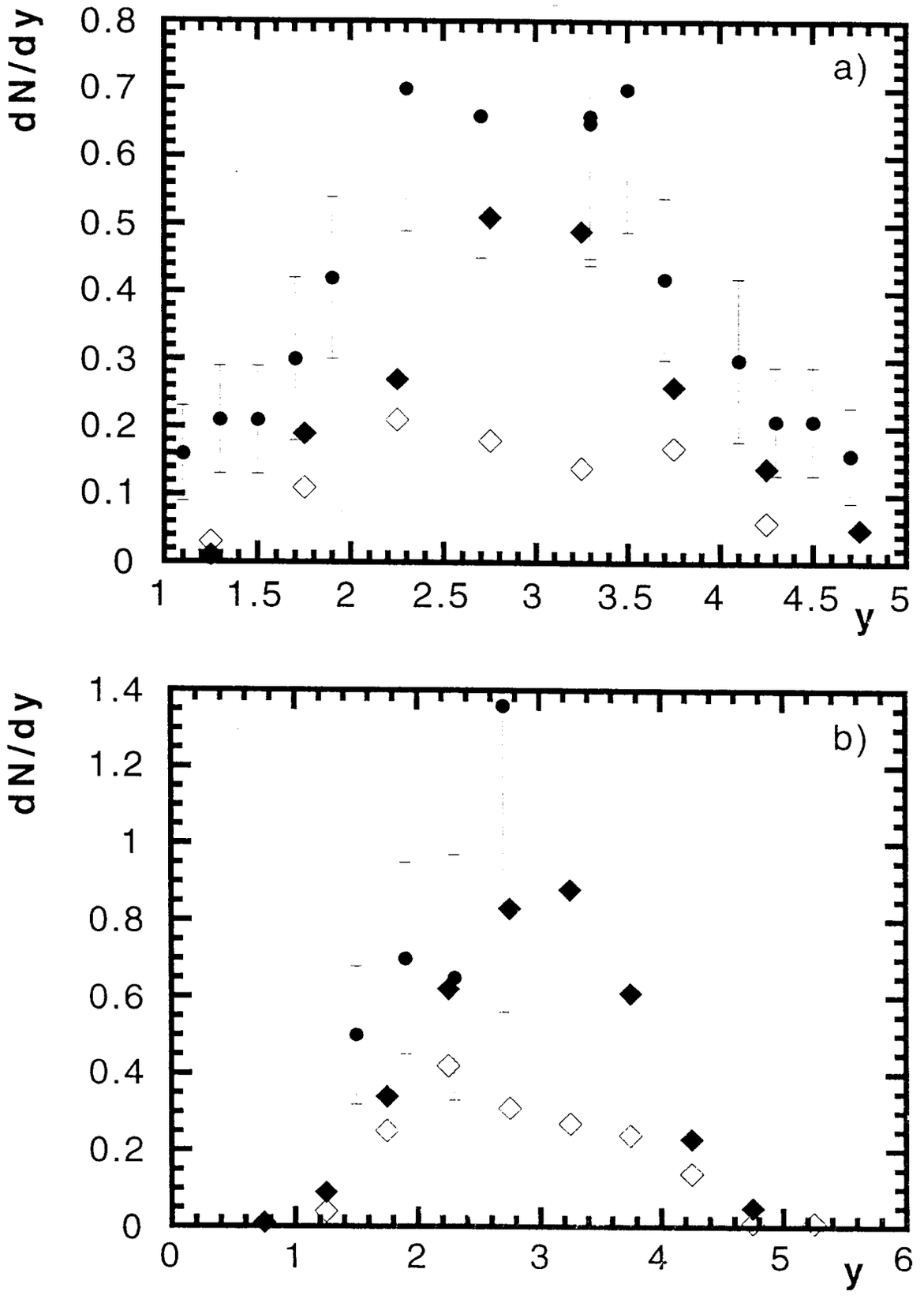
dN/dy
0.8
0.7
0.6
0.5
0.4
0.3
0.2
0.1
0
a)
1
1.5
2
2.5
3
3.5
4
4.5
5
y
dN/dy
1.4
1.2
1
0.8
0.6
0.4
0.2
0
b)
0
1
2
3
4
5
6
y

Fig. 4

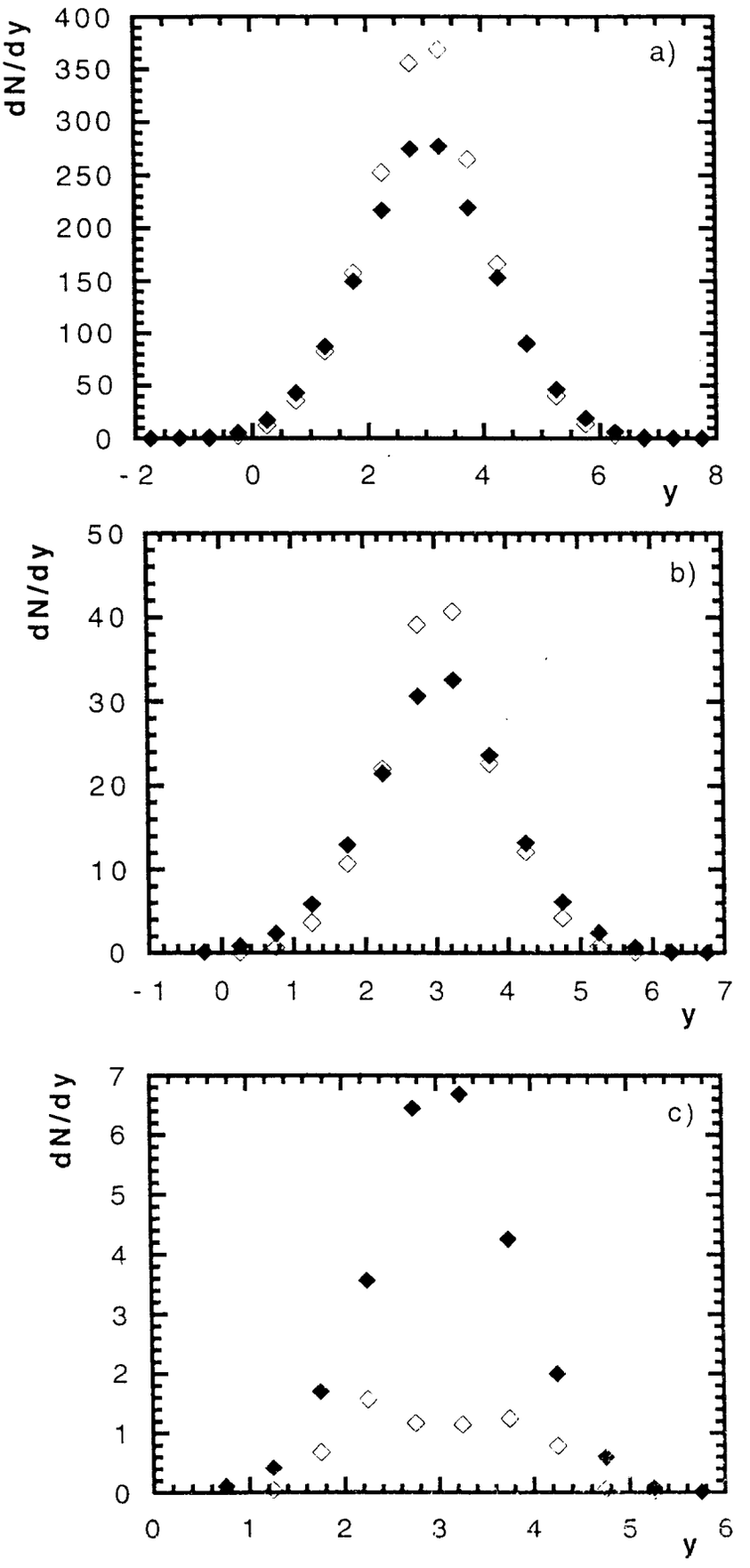
dN/dy
a)
400
350
300
250
200
150
100
50
0
-2
0
2
4
6
8
y
dN/dy
b)
50
40
30
20
10
0
-1
0
1
2
3
4
5
6
7
y
dN/dy
c)
7
6
5
4
3
2
1
0
0
1
2
3
4
5
6
y

Fig. 5